

Relationship Between Voids and Interlaminar Shear Strength of Polymer Matrix Composites

Kenneth J. Bowles and Stephen Frimpong
Lewis Research Center
Cleveland, Ohio

Prepared for the
36th International SAMPE Symposium and Exhibition
sponsored by the Society for the Advancement of Materials
and Process Engineering
San Diego, California, April 15-18, 1991



(NASA-TM-103643) RELATIONSHIP BETWEEN VOIDS
AND INTERLAMINAR SHEAR STRENGTH OF POLYMER
MATRIX COMPOSITES (NASA) 20 p CSCL 11D

N91-13495

Unclass

G3/24 0317947

RELATIONSHIP BETWEEN VOIDS AND INTERLAMINAR SHEAR STRENGTH OF
POLYMER MATRIX COMPOSITES

Kenneth J. Bowles and Stephen Frimpong
National Aeronautics and Space Administration
Lewis Research Center
Cleveland, Ohio 44135-3191

ABSTRACT

This paper describes the effect of voids on the interlaminar shear strength of a polyimide matrix composite system. The AS4 graphite/PMR-15 composite was chosen for study because this system can be readily processed by using the standard specified cure cycle to produce void-free composites and because preliminary work in this study had shown that the processing parameters of this resin matrix system can be altered to produce cured composites of varying void contents. Thirty-eight 12-ply unidirectional composite panels were fabricated for this study. A significant range of void contents (0 to 10 percent) was produced. The panels were mapped, ultrasonically inspected, and sectioned into interlaminar shear, flexure, and fiber content specimens. The density of each specimen was measured and interlaminar shear and flexure strength measurements were then made. The fiber content was measured last. The results of these tests were evaluated by using ultrasonic results, photomicrographs, statistical methods, theoretical relationships derived by other investigators, and comparison of the test data with the Integrated Composite Analyzer (ICAN) computer program developed at the Lewis Research Center for predicting composite ply properties. The testing program is described in as much detail as possible in order to help others make realistic comparisons.

KEYWORDS: Composites; Voids; Interlaminar shear; Graphite fibers; Polyimides; Density

1. INTRODUCTION

Fiber-reinforced polymer matrix composites are now being used as production materials of construction in the aircraft, aerospace, and automotive industries. The successful use of these materials is based on the ability to exploit their high-strength, high-modulus, and low-density characteristics. However, it is also contingent on the ability to consistently produce structures that satisfy the requirements established by the design engineer.

In general, for most fiber-resin systems, one of the component variables that is dependent on manufacturing techniques and curing procedures is void content. The void content, in turn, has a marked effect on composite interlaminar shear strength (ILSS) (1,2), which has a significant effect on compressive strength, impact resistance, and fatigue life (3-5). The consistent production of void-free composite structures by a full-scale production facility may not be guaranteed for all fiber-resin systems. For this reason the effect of voids on the mechanical properties of composite materials must be considered, investigated, and understood so that allowable deviations from void-free conditions can be determined and specified when necessary.

This paper describes the effect of voids on the interlaminar shear strength of a polyimide matrix composite system. The AS4 graphite/PMR-15 composite was chosen for study for the following reasons:

- (1) This system can be readily processed using the standard specified cure cycle to produce void-free composites.

- (2) Preliminary work in this study has shown that the processing parameters of this resin matrix system can be altered to produce cured composites of varying void contents.

Thirty-eight 12-ply unidirectional composite panels were fabricated for this study. A significant range of void contents (0 to 10 percent) was produced. The panels were mapped, ultrasonically inspected (6), and sectioned into interlaminar shear, flexure, and fiber content specimens. The density of each specimen was measured and interlaminar shear and flexure strength measurements were then made. The fiber content was measured last.

The results of these tests were evaluated by using ultrasonic results (6,7), photomicrographs, statistical methods, and theoretical relationships derived by other investigators. The data were also compared with calculated values from the Integrated Composite Analyzer (ICAN) computer program

developed at the Lewis Research Center for predicting composite ply properties (8). The testing program is described in relatively great detail to allow others to compare these results with comparable data from other researchers.

2. EXPERIMENTAL PROCEDURES

2.1 Monomeric Reactant Solution The monomers used in this study are listed in Table 1. The monomethyl ester of 5-norbornene-2,3 dicarboxylic acid (NE) and 4,4'-methylenedianiline (MDA) were obtained from commercial sources. The dimethyl ester of 3,3',4,4'-benzophenonetetracarboxylic acid (BTDE) was synthesized as described in (9). Reactant solutions were prepared at a solids loading of 50 percent by weight in methanol. The stoichiometry of the reactants was adjusted to give a formulated molecular weight of 1500.

2.2 Composite Fabrication Thirty-eight 12-ply unidirectional laminates were fabricated for this study. Each ply was cut from prepreg sheets that were made by drum-winding Hercules AS4 graphite fibers and impregnating the fibers with the PMR-15 monomer solution. Fiber tows with 10 000 fibers per tow were wound with a pitch of 3 tows per centimeter (7 tows per inch). The fiber was impregnated with an amount of monomer solution required to yield a cured ply thickness of 0.018 cm (0.08 in.) and a fiber content of about 60 wt % if no resin flow occurred. The prepreg was air dried for 1 hour on the drum. It was then heated to 49 °C (120 °F) on the drum for an additional hour. This drying procedure reduced the volatiles content to about 10 percent by weight. The result was a drapeable, nontacky prepreg.

After drying, the prepreg sheets were removed from the drum and cut into 7.62- by 25.40-cm (3- by 10-in.) plies with the fibers aligned with either the 25.40-cm (10-in.) direction (28 unidirectional laminates were fabricated with this orientation) or the 7.62-cm (3-in.) direction (11 unidirectional laminates). For either orientation, 12 plies were stacked unidirectionally and imidized in a rectangular preforming cup for 3 hours at 121 °C (250 °F) and an applied pressure of 2.07×10^{-3} MPa (0.3 psi). The final cure procedure involved heating a matched metal die mold to 232 °C (450 °F) and inserting the imidized preformed stack. The preform was contained in the die and held under press contact pressure for 10 minutes. After this initial dwell time the cure pressure (which varied from specimen to specimen) was applied to the die, and the mold temperature was increased to 315 °C (600 °F) at a rate of 5.5 deg C (10 deg F) per minute. When 316 °C (600 °F) was reached, the temperature and pressure were held for 1 hour. The cure pressures used in this study are presented in Fig. 1. These cure

pressures produced a significant range of void contents and fiber/resin ratios. The properties of the fiber and the matrix materials are listed in Table 2.

The laminates were made in three groups: laminates 1 to 12, 20 to 30, and 31 to 48. Some laminates were discarded, so that the number of laminates reported is 38 and not 42.

2.3 Specimen Description Figure 2 is a mapping of a typical laminate that was fabricated with the fibers oriented in the longitudinal (25.4 cm; 10 in.) direction. These unidirectional panels are designated as panels 1 to 12 and 31 to 48. Panels 37, 43, and 45 were not tested. Panels 20 to 30 contained fibers oriented in the 7.62-cm (3-in.) direction.

2.4 Ultrasonic Scanning Before the 38 laminates were cut into test samples, they were mapped by two different ultrasonic procedures. Each laminate underwent a black-white C-scan and an amplitude scan. The scanning was done with the panels immersed in distilled water. They were positioned between two 2.5-MHz transducers - one sending and the other receiving. These laminates were subjected to an extensive ultrasonic examination. In addition to the mapping, spot attenuation and velocity measurements were made by using contact ultrasonics. Stress wave simulation measurements were made on each laminate. The ultrasonic evaluation of these specimens is described in detail elsewhere (6,7).

2.5 Composite Density Density measurements were made by a water immersion technique in accordance with ASTM D-792. The density measurement and void content values are listed in Table 3 along with the standard and average standard deviations for the total of 38 laminates and also for the three groups (1 to 12, 20 to 30 and 31 to 48).

2.6 Fiber Content The corresponding fiber volume fractions were calculated from the measured density data by using the fiber and matrix densities. They can be compared with the spread of the actual fiber content data that were measured by the acid digestion technique and are presented in Table 4.

At least two short-beam shear specimens from each of the 38 laminates were subjected to the H_2SO_4/H_2O_2 digestion technique (ASTM D-3171) to measure the fiber content. The measured values are presented in Table 4, along with the differences between the two measurements. In addition one specimen from each of the laminates designated as 31 to 48 were sent to an independent testing laboratory for fiber content and void content measurement. These values are also listed in Table 4. The sixth column lists the differences between the maximum and minimum measurements as a percentage of the average content from the fifth column of the table.

2.7 Void Content The void content of each of the specimens was calculated from the measured fiber content and density values (Fig. 1 and Table 3). The calculations were made by using the following formula:

$$V_v = 1 - D_c(V_f/D_f + V_r/D_r) \quad (1)$$

where

V_v void volume fraction
 D_c composite density
 V_f fiber weight fraction
 D_f fiber density
 V_r resin weight fraction
 D_r resin density

The fiber density used was 1.799 g/cm³ (vendor's measurement). The resin density was measured by water immersion (ASTM D-792) and was 1.313 g/cm³. The reliability of the void content determination is discussed in (10). The method is not accurate for void contents less than roughly 1 percent. For calculated void contents in this range, metallography was used to make a reasonable estimate of the void content.

2.8 Metallography Metallographic samples were taken from the laminates. The samples were mounted, polished, and photographed at different magnifications, X30 to X160, to confirm the void size distribution and shape. Typical photomicrographs are presented in Figs. 3 and 4.

2.9 Interlaminar Shear Strength All interlaminar shear tests were made at room temperature in accordance with ASTM D-2433 by using a three-point loading fixture with a constant span-to-depth ratio of 5. The rate of loading was 0.02 cm/sec (0.05 in./min). The number of specimens of each laminate that were tested varied from 8 to 20. Thickness varied from 0.23 to 0.25 cm (0.09 to 0.10 in.). These specimens were all 0.508 cm (0.2 in.) wide. The results of these tests are presented in Table 5.

3.0 ANALYSIS OF RESULTS

3.1 Composite Quality Figure 3 shows composite samples 35, 34, and 40, which contain 1.25, 3.9, and 12.1 percent voids, respectively. The specimens were sectioned perpendicular to the direction of the reinforcement. The voids are shown as holes between the fibers with those of Fig. 3(c) being circular. In Fig. 4 the same specimens are shown but with the sectioning oriented parallel to the reinforcement direction. In this view the voids are shown as long slits. From the information presented by these two figures, it appears that the voids are more or less cylindrical and situated between the plies. The specimens with the low void contents do

not have their voids evenly distributed throughout the volume of the composites. In the case of specimen 35 (1.25 percent voids) the voids are not evenly distributed among the ply interfaces but are apparently segregated at one portion of the composite cross section. The fractions of voids were estimated, from the voids shown in Fig. 4, by measuring the relative lengths of voids to matrix. They comprise 44, 22, and 36 percent of the interlaminar matrix material, respectively. It does appear that the void distribution may become more homogeneous as the void content increases (Fig. 4(c)). In considering the low-void-content composites, one can infer that the interlaminar shear strength of the composite is dependent on the location of the voids. If they are located near the outer surfaces, there should be no effect on the shear strength, since theoretically the shear stresses increase from zero at the specimen surfaces to a maximum at the neutral plane. If they are located near the inner high-shear-stress areas, the voids can cause premature failure (lower calculated failure stresses).

As previously indicated, the ultrasonic examinations of the specimens are presented in detail elsewhere (6,7). It was found that an ultrasonic-acoustic technique using the measurement of the stress wave factor was effective in evaluating the interlaminar shear strength of fiber-reinforced composites. The details of this portion of the study can be obtained from these references.

3.2 Composite Densities and Fiber Content Composite densities and changes in fiber volume fractions are presented in Table 3. The density listed for each of the 38 specimens is the numerical average calculated for the number of specimens listed in the table for each of the three groups of specimens. A total of 403 density measurements were made. The average standard and standard deviations were calculated for each group of specimens and for the total of 38 specimens and are included in the table. All laminates except 5, 36, and 40 had measured densities with standard deviations of less than 1 percent. The corresponding changes in fiber volume fractions were calculated by using the following relationship:

$$\Delta V_f = \Delta D_c (1 - V_v) / 0.486 \quad (2)$$

where

ΔV_f change in fiber volume fraction

ΔD_c change in composite density

Actual differences between composite fiber volume fractions for each laminate are also shown in Table 3. They have been calculated as the difference between the maximum and minimum fiber volume fractions measured by the acid digestion technique for each group of specimens. The measured fiber

volume fractions are presented in Table 4. The majority of the measurements were made at the Lewis Research Center, but a series of digestions were also performed at a commercial laboratory and are listed in the table. The standard deviations between the values measured at Lewis and those measured at the private laboratory are also tabulated in Table 4. The calculated standard deviations for these values, which were measured by the acid digestion technique, are about 2.5 times the values converted to fiber volume fractions by calculations from the density data. The average difference is about 3 percent. The number of specimens digested was 64. No trends appear in the data in Table 3, as indicated by the average standard deviations of the three groups, or in Table 4. The average standard deviation of the density measurements in Table 3 is 0.59 percent; the standard deviation of the fiber content, as measured by acid digestion (Table 4), is 2.02 percent. It is evident that the density measurements by water immersion produced more consistent results than the densities calculated from fiber fraction content data measured by the acid digestion technique. The digestion measurements are necessary for calculating the void contents.

3.3 Void Content In spite of the variations in the fiber content measurements shown in Table 4, the calculated void contents in Table 3 show good agreement within each group of specimens. Except for specimen 36, they all appear to be within a percentage point of each other.

The cure pressure for each laminate is included in Fig. 1. At each end of the pressure spectrum investigated, the void content increased. At the low end of <1.4 MPa (<200 psi), the reason for void increase was probably the lack of pressure needed to sweep out the volatiles and the air pockets within the fluidized matrix. Apparently when higher pressures >6.9 MPa are applied (>1000 psi), volatiles and air may be trapped within the laminate, resulting in void formation. When the cure pressures are held between 5.5 and 1.4 MPa (800 and 200 psi), void-free laminates are produced. There does not seem to be a clear indication of differences due to fiber orientation (0° or 90°) in void content or mechanical property variations within a group of laminates cured under the same pressure for this size of specimen.

3.4 Interlaminar Shear Strength Table 5 contains the data from the 409 individual short-beam shear tests from the 38 groups of specimens. Standard deviations of each of the groups are presented both in megapascals (or kips per square inch) and in percent of the average interlaminar shear strength (ILSS) value along with the total average and total standard deviations of the 38 laminates. The total average standard deviation for the whole group is 4.88 percent. For a 99.9-percent confidence factor, the ILSS values are grouped within a ± 7.5 -percent band as determined by the 3σ value. The values that are outside this limit are those for the specimens

numbered 31, 36, 39, and 40. Examination of Fig. 1 and Tables 3 and 4 does not reveal a trend for such behavior. For the purposes of this report the specimens were divided into three groups corresponding to their time of fabrication and testing. The first group (1 to 12) contains only void-free composites. The second group (20 to 30) includes laminates with void contents from 0 to 6 percent. The third group (31 to 48) contains laminates with void contents from 6 to 10 percent. As can be seen from table 5, as the void content increased, the average standard deviation increased from 3.7 to 4.1 percent and then to 8.1 percent. The large standard deviations in the ILSS measurements, as compared with the standard deviations in the density measurements, are due to random defects in the composites (such as voids) that at times are positioned so that they cause premature failure. As previously discussed, the distribution of defects is illustrated by microscopic examination, as shown in Figs. 3 and 4. Although the void content of specimen 40 is 12.1 percent, these voids are distributed evenly throughout the sample. Specimen 35, with a void content of 1.25 percent, has the voids segregated primarily between the plies.

3.5 ILSS Correlation With Void and Fiber Content Figure 5 shows the good correlation between the composite ILSS and the composite density. The scatter is greatest at the low-density end of the plot. This relationship is shown in both a linear and power equation configuration in the figure. These equations are well suited, since the data indicate that the composite density measurements are more consistent than the fiber fraction data from acid digestion. The measured ILSS data were fitted to the two types of equations with composite density as the dependent variable. The density is expressed in terms of the fiber and void fractions in order to allow comparison of the equations with equations from the literature (11). The relationship used is

$$D_c = (1 - V_v)(0.486V_f + 1.33) \quad (3)$$

The consensus of opinion is that there are two possible void configurations in composites: cylindrical and spherical. The equations theoretically derived for cylindrical and spherical voids and published in (11) are

$$\text{Cylindrical:} \quad ILSS_r = \left[1 - \frac{4V_v}{3.14(1 - V_{fv})} \right]^{1/2} \quad (4)$$

$$\text{Spherical:} \quad ILSS_r = 1 - \frac{3.1416}{4} \left[\frac{6V_v}{3.1416(1 - V_{fv})} \right]^{2/3} \quad (5)$$

where V_{fv} is the fiber volume fraction of the composite with voids and $ILSS_r$ is the ILSS of the composite with voids relative to that of the void-free composite.

The power equation produced the best fit in respect to the calculated correlation coefficients. The R^2 values were 0.45 and 0.86 for the linear and power regressions, respectively. When only those data points from specimens that contained no voids were analyzed, the R^2 value for the linear equation fit increased to 0.593. The linear and power relationships between the ILSS and the composite density are as follows:

$$ILSS = 2.307(1 - V_v)(0.486V_f + 1.313) - 2.702 \quad (6)$$

$$ILSS = 2.035(1 - V_v)(0.486V_f + 1.313)^{4.46} \quad (7)$$

Equation (7) was used to generate the sensitivity analyses displayed in Table 6. Equation (7) was selected to represent the measured values because it has a much better R^2 value than Equation (6) and because it is similar mathematically to the theoretically derived Equations (4) and (5). However, Equation (6) can be used to quickly calculate a reasonable value for the ILSS of a composite with a known density. Tables 7 and 8 contain sensitivity analyses calculated by using Equations (4) and (5) for composites with cylindrical and spherical voids. The values were calculated as percent of the void-free laminate ILSS.

The sensitivity analysis in Table 6 indicates that there was about an 11-percent decrease in composite ILSS when fiber content decreased from 60 to 50 percent. An 11 percent increase in void content is reflected as a 40-percent drop in composite ILSS. The models presented in Tables 7 and 8 show a larger effect from fiber content changes on the ILSS and a significantly greater effect from void content changes than shown in Table 6.

The data for four different types of composites with 60-percent fiber volume fraction are plotted in Fig. 6. The types of data are as follows:

- (1) Measured data
- (2) Spherical void content
- (3) Cylindrical void content
- (4) Modeled by ICAN (11)

It is evident that the measured data from this study closely approximate the curve produced with values calculated by using the relationship between ILSS and spherical void content. The models suggest that cylindrical voids would produce lower values of ILSS. The close correlation between the measured data and the curve for a composite with spherical voids does not support the metallographic evidence in Figs. 3 and 4 which caused us to conclude that the voids in the laminates studied were cylindrical. The

equation incorporated in the ICAN program is similar to that of Equation (4) for cylindrical voids. The curves shown for cylindrical void content and composite modeled by ICAN do lie close together. The ILSS data from this study indicate that the voids acted as spherical voids in reducing the ILSS. This significant inconsistency can only be explained by conjecture. It may be that the voids can be considered as small delaminations or cracks or of some other configuration that when modeled gives the same type of equation as the spherical void model.

From the results of this study the ICAN program can be improved for the laminates described herein by assuming spherical void behavior rather than cylindrical void behavior as currently assumed. In addition to the correction for void shape we found that the ICAN-predicted ILSS values for the composite material studied in this program were almost one-half the measured values. Attempts by other investigators to calculate the shear strength have been unsuccessful (1). Measured composite shear strengths have been found to exceed the shear strength of the matrix. Comparison of the ILSS data predicted by ICAN and shown in Table 9 with the data in Tables 2 and 5 show this. It would seem necessary to include a factor for the degree of interfacial bonding between the fiber and the matrix or to experimentally confirm the matrix and fiber shear properties used in any model derived for predicting the ILSS of polymer matrix composite materials.

4.0 SUMMARY

An extensive study was conducted to relate the interlaminar shear strength of AS4/PMR-15 unidirectional composites with both fiber and void contents. Composite densities and fiber contents were measured along with the interlaminar shear strengths of 39 different composite laminates. Void contents were calculated and the void geometry and distribution were noted by using microscopic examination techniques such as those used in metallography. The measured data were fitted to various types of curves by using regression analyses. The empirical correlations between strength and composite density were good.

The most logical relationship between ILSS and density seems to be the power equation (Eq. (7)). This logic is based on the close resemblance to the theoretically derived equations from (11) and the relatively good fit of the data. Comparison of the values calculated from Equation (7) with those calculated from Equations (4) and (5) showed a good correlation between the empirically derived relationship from this study and the ILSS values predicted by the spherical void model. High-magnification photographs of polished surfaces indicated that most voids were cylindrical.

The ICAN program developed at the Lewis Research Center predicts a relationship based on cylindrical voids and thus predicts lower ILSS values than the measured data. No model was found that accurately predicts the absolute value of ILSS for the AS4/PMR-15 composite.

More scatter appeared in the composite strength values as the void content increased. Composite fiber contents calculated from density measurements were more consistent than those measured by the acid digestion technique. The distribution of voids within the composites became more homogeneous as the void content increased. In those laminates with low void content the voids appeared to be more segregated in one area of the laminate.

The results of this study indicate that void-free composites can be processed at pressures greater than 1.4 MPa (200 psi) and less than 6.9 MPa (1000 psi).

5.0 REFERENCES

1. Hancox, N.L., "The Effects of Flaws and Voids on the Shear Properties of CFRP," Journal of Materials Science, Vol. 12, No. 5, 1977, pp. 884-892.
2. Yoshida, H., Ogasa, T., and Hayashi, R., "Statistical Approach to the Relationship Between ILSS and Void Content of CFRP," Composites Science and Technology, Vol. 25, No. 1, 1986, pp. 3-18.
3. Kunz, S.C. and Beaumont, P.W.R., "Microcrack Growth in Fiber-Epoxy Resin Systems During Compressive Fatigue," Fatigue of Composite Materials, ASTM STP569, 1975, pp. 71-91.
4. Greszczuk, L.B., "Compressive Strength and Failure Modes of Unidirectional Composites," Analysis of the Test Methods for High Modulus Fibers and Composites, ASTM STP-521, 1973, pp. 192-217.
5. Bowles, K.J., "The Correlation of Low Velocity Impact Resistance of Graphite-Fiber-Reinforced Composites With Matrix Properties," Composite Materials: Testing and Design (Eighth Conference), J.D. Whitcomb, ed., ASTM STP-972, 1988, pp. 124-142.
6. Vary, A. and Bowles, K.J., "Ultrasonic Evaluation of the Strength of Unidirectional Graphite-Polyimide Composites," NASA TM X-73646, 1977.

7. Vary, A. and Bowles, K.J., "An Ultrasonic-Acoustic Technique for Nondestructive Evaluation of Fiber Composite Quality," Polymer Engineering and Science, Vol. 19, No. 5, Apr. 1979, pp. 373-376.
8. Murthy, P.L.N. and Chamis, C., "Integrated Composites Analyzer (ICAN): Users and Programmers Manual, NASA TP-2515, 1986.
9. Serafini, T.T. and Vannucci, R.D., "Tailormaking High Performance Graphite Fiber Reinforced PMR Polyimides," Reinforced Plastics-Milestone 30, Society of the Plastics Industry, 1975, pp. 14-E1 to 14-E5. (Also, NASA TM X-71616).
10. Cilley, E., Roylance, D., and Schneider, N., "Methods of Fiber and Void Measurement in Graphite/Epoxy Composites," Composite Materials Testing and Design (Third Conference), ASTM STP-546, 1974, pp. 237-249.
11. Greszczuk, L.B., "Effect of Voids on Strength Properties of Filamentary Composites," Proceedings, 22nd Annual Meeting of the Reinforced Plastics Division, Society of the Plastics Industry, 1967, pp. 20-A.1 to 20-A.10.

TABLE 1. - MONOMERS USED FOR PMR-15 POLYIMIDE

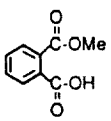
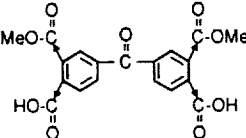
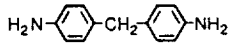
Structure	Name	Abbreviation
	Monomethyl ester of 5-norbornene-2,3-dicarboxylic acid	NE
	Dimethyl ester of 3,3',4,4'-Benzophenonetetracarboxylic acid	BTDE
	4,4'-Methylenedianiline	MDA

TABLE 2. - CONSTITUENT PROPERTIES

[From reference 11.]

Property	As graphite	PMR-15 matrix
Logitudinal tensile modulus, GPa (Msi)	213.7(31)	3.2(0.470)
Transverse tensile modulus, GPa (Msi)	13.7(2)	
Shear modulus 12, GPa (Msi)	13.7(2)	1.1(0.173)
Shear modulus 23, GPa (Msi)	6.8(1)	
Poisson's ratio	0.3	0.36
Tensile strength, MPa (ksi)	3033.8(440)	55.8(8.1)
Compression strength, MPa (ksi)	-----	11.37(16.5)
Shear strength, MPa, (ksi)	-----	55.8(8.1)
Density, g/cm ³	1.799	1.313

TABLE 3. - DENSITY OF COMPOSITES

Specimen	Number of samples	Density, g/cm ³	Standard deviation		Calculated deviation in fiber fraction, percent	Measured deviation of fiber fraction, percent	Calculated void content (measured data), percent
			g/cm ³	Percent			
1	8	1.595	10.5x10 ³	0.66	1.35	7.48	0,1.6
2		1.587	2.9	.18	.38	.04	
3		1.575	5.5	.35	.72	1.17	0,0
4		1.613	8.4	.52	1.07	1.11	1.6,1.4
5		1.521	18.9	1.24	2.55	2.08	0,0
6		1.622	11.3	.70	1.43	1.51	2.2,2.8
7		1.566	13.8	.88	1.81	15.57	0,0
8		1.573	8.0	.51	1.05	.12	0,0
9		1.596	5.5	.34	.71	4.99	1.4,0
10		1.581	8.0	.51	1.04	1.76	0,0
11		1.583	13.5	.85	1.75	6.42	0,1.6
12	12	1.623	13.5	.83	1.71	3.27	3.2,2.4
20	8	1.581	5.5	.35	.72	.05	0,0,0
21	20	1.569	15.2	.97	1.97	.38	0,1.0
22	18	1.552	10.0	.64	1.31	2.10	0,0,0
23	20	1.558	4.7	.30	.61	7.99	1.5,1.6,0
24	20	1.517	5.3	.35	.69	4.09	5.0,4.5,4.8
25	20	1.573	13.9	.88	1.82	1.51	1.9,1.7,0
26	10	1.500	5.9	.39	.77	.64	4.7,4.8,5.4
27	20	1.477	5.1	.35	.67	6.01	6.4,5.9,6.4
28	19	1.529	9.5	.62	1.25	5.30	2.8,2.4,2.8
29	20	1.510	7.4	.49	.97	1.57	4.5,3.8,4.3
30	8	1.575	5.5	.35	.72	1.07	0,0,0
31	8	1.568	8.2	.52	1.08	2.78	0,0
32	6	1.561	4.1	.26	.54	1.01	0,0
33	8	1.570	4.5	.29	.59	.91	0,0
34		1.515	10.0	.66	1.31	2.92	4.2,4.0
35		1.539	6.2	.40	.82	1.53	1.2,1.6
36		1.461	22.9	1.57	2.97	1.00	6.1,10.1
38		1.443	5.7	.40	.75	4.07	7.9,8.6
39		1.456	11.9	.82	1.57	1.32	7.1,6.7
40		1.356	24.8	1.83	3.31	.68	12.5,11.7
41		1.453	10.4	.72	1.36	2.68	7.0,10.2
42		1.417	7.4	.52	.98	3.37	9.2,9.9
44		1.561	4.2	.27	.55	5.07	
46		1.574	5.4	.34	.71	4.93	
47		1.464	4.2	.29	.55	4.91	5.8,7.1
48		1.469	5.4	.37	.71	2.70	

Total average standard deviation	0.59
Total standard deviation	0.35
Specimens 1 to 12:	
Average standard deviation	0.63
Standard deviation	0.28
Specimens 20 to 30:	
Average standard deviation	0.52
Standard deviation	0.22
Specimens 31 to 48:	
Average standard deviation	0.62
Standard deviation	0.46

TABLE 4. - FIBER CONTENT MEASUREMENTS BY ACID DIGESTION TECHNIQUE

Specimen	Lewis Research Center					Independent testing laboratory measurement, percent	Lewis average minus independent measurement, percent
	Measurement, percent			Average, percent	Difference (max. to min.), percent		
	1	2	3				
1	53.49	58.13	-----	56.04	4.19	-----	-----
2	54.23	54.25	-----	54.24	.02	-----	-----
3	54.38	53.75	-----	54.07	.63	-----	-----
4	57.88	57.24	-----	57.56	.64	-----	-----
5	49.41	50.45	-----	49.93	1.04	-----	-----
6	59.93	60.84	-----	60.39	.91	-----	-----
7	54.49	46.62	-----	50.56	7.87	-----	-----
8	51.71	51.77	-----	51.74	.06	-----	-----
9	57.28	54.49	-----	55.89	2.79	-----	-----
10	53.09	54.03	-----	53.56	.94	-----	-----
11	51.25	54.65	-----	52.95	3.40	-----	-----
12	62.79	60.77	-----	61.78	2.02	-----	-----
19	55.92	55.90	56.17	55.30	.48	-----	-----
21	58.38	58.64	56.28	57.77	4.02	-----	-----
22	54.85	53.71	54.08	54.21	2.08	-----	-----
23	55.49	55.94	51.58	54.34	7.79	-----	-----
24	59.66	57.26	58.12	58.35	4.13	-----	-----
25	57.77	58.64	57.99	57.99	1.48	-----	-----
26	55.29	55.49	55.14	55.31	.63	-----	-----
27	56.38	53.09	53.90	54.46	5.84	-----	-----
28	54.63	53.68	51.77	53.36	5.24	-----	-----
29	55.83	58.03	54.96	56.27	5.29	-----	-----
30	55.36	55.15	55.74	55.42	1.06	-----	-----
31	51.29	52.74	-----	52.02	1.45	52.20	-0.19
32	50.57	51.08	-----	50.83	.51	50.00	.83
33	52.38	52.86	-----	52.62	.48	53.80	-1.18
34	50.10	51.59	-----	50.85	1.49	51.19	-.34
35	51.36	50.58	-----	50.97	.78	50.63	.34
36	48.75	48.27	-----	48.51	.48	46.89	1.62
38	46.23	48.16	-----	47.20	1.93	47.70	-.50
39	48.31	48.95	-----	48.63	.64	48.42	.21
40	43.67	43.96	-----	43.82	.29	41.47	2.64
41	47.35	48.64	-----	48.00	1.29	48.60	-.61
42	44.50	46.03	-----	45.27	1.53	45.79	-.52
44	48.61	51.71	-----	49.89	2.56	51.60	-1.71
46	51.76	54.40	-----	53.08	2.64	54.60	-1.52
47	46.42	48.78	-----	47.60	2.36	48.97	-1.37
48	47.87	49.19	-----	48.53	1.32	49.37	-.84

	Lewis difference (max. to min.), percent	Lewis average minus independent measurement, percent
Average standard deviation	2.17	-0.21
Standard deviation	2.02	1.16
Specimens 1 to 12:		
Average standard deviation	2.04	-----
Standard deviation	2.17	-----
Specimens 19 to 30:		
Average standard deviation	2.34	-----
Standard deviation		-----
Specimens 31 to 48:		
Average standard deviation	1.32	-----
Standard deviation	.76	-----

TABLE 5. - ROOM-TEMPERATURE INTERLAMINAR SHEAR STRENGTH DATA FOR
UNIDIRECTIONAL COMPOSITES

Specimen	Number of samples	Interlaminar shear strength		Standard deviation		
		MPa	ksi	MPa	psi	Percent
1	8	122.0	17.7	6.0	8.7×10^{-2}	4.92
2		108.9	15.8	1.9		1.77
3		111.0	16.1	4.6		4.16
4		108.9	15.8	2.8		2.53
5		91.0	13.2	3.2		3.48
6		113.8	16.5	3.7		3.27
7		104.8	15.2	3.6		3.42
8		108.3	15.7	3.3		3.06
9	9	112.4	16.3	5.2	7.6	4.66
10	10	108.3	15.7	4.5	6.5	4.14
11	11	110.3	16.0	4.4	6.4	4.00
12	12	124.8	18.1	6.0	8.7	4.81
19	8	113.8	16.5	4.9	7.1	4.30
21	20	111.7	16.2	5.2	7.5	4.63
22	18	97.3	14.2	3.7	5.3	3.73
23	20	102.7	14.9	4.2	6.1	4.09
24	20	90.3	13.1	2.4	3.5	2.67
25	20	114.5	16.6	3.4	4.9	2.95
26	10	83.4	12.1	3.2	4.6	3.80
27	20	80.7	11.7	2.1	3.1	2.65
28	19	97.2	14.1	9.9	14.4	10.21
29	20	89.6	13.0	3.2	4.6	3.54
30	8	107.6	15.6	3.0	4.4	2.82
31	↓	94.5	13.7	12.5	18.1	13.21
32		105.5	15.3	4.0	5.8	3.79
33		107.6	15.6	3.6	5.2	3.33
34		90.3	13.1	4.7	6.8	5.19
35		101.4	14.7	3.2	4.7	3.20
36		66.2	9.6	6.1	8.9	9.27
38		61.4	8.9	3.6	5.2	5.84
39		64.8	9.4	6.5	9.4	10.00
40		66.9	9.7	7.6	11.0	11.34
41		66.2	9.6	3.4	4.9	5.10
42		77.9	11.3	2.8	4.1	3.63
44		106.2	15.4	3.6	5.2	3.38
46		103.4	15.0	5.9	8.5	5.67
47		73.8	10.7	5.9	8.5	7.94
48		75.8	11.0	3.9	5.6	5.09

	Standard deviation		
	MPa	psi	Percent
Total average standard deviation	4.5	6.5×10^{-2}	4.88
Total standard deviation	2.1	3.1	2.60
Specimens 1 to 12:			
Average standard deviation	----	-----	3.70
Standard deviation	----	-----	.91
Specimens 19 to 30:			
Average standard deviation	----	-----	4.13
Standard deviation	----	-----	2.03
Specimens 31 to 48:			
Average standard deviation	----	-----	8.12
Standard deviation	----	-----	3.09

TABLE 6. - SENSITIVITY ANALYSIS OF INTERLAMINAR SHEAR STRENGTH
FOR COMPOSITES WITH VOIDS AND FIBER CONTENT AS VARIABLES
[Calculated by using equation (7).]

Void volume, V_v , percent	Fiber volume, V_f , percent										
	60	59	58	57	56	55	54	53	52	51	50
	Interlaminar shear strength, percent of initial ILSS										
0	100	99	97	96	95	93	92	91	90	88	87
1	96	94	93	92	91	89	88	87	86	85	83
2	91	90	89	88	87	85	84	83	82	81	80
3	87	86	85	84	83	82	80	79	78	77	76
4	83	82	81	80	79	78	77	76	75	74	73
5	80	78	77	76	75	74	73	72	71	70	69
6	76	75	74	73	72	71	70	69	68	67	66
7	72	71	70	69	69	68	67	66	65	64	63
8	69	68	67	66	65	64	64	63	62	61	60
9	66	65	64	63	62	61	61	60	59	58	57
10	63	62	61	60	59	58	58	57	56	55	54
11	59	59	58	57	56	56	55	54	53	53	52

TABLE 7. - CYLINDRICAL VOID MODEL SENSITIVITY ANALYSIS OF ILSS AS FUNCTION OF FIBER AND VOID CONTENT
[Calculated by using equation (4).]

Void volume, V_v , percent	Fiber volume, V_f , percent										
	60	59	58	57	56	55	54	53	52	51	50
	Interlaminar shear strength, percent of initial ILSS										
0	100.0000	100.0000	100.0000	100.0000	100.0000	100.0000	100.0000	100.0000	100.0000	100.0000	100.0000
1	82.2898	82.5019	82.7066	82.9042	83.0952	83.2800	83.4588	83.6320	83.7999	83.9627	84.1207
2	75.1318	75.4226	75.7035	75.9750	76.2376	76.4917	76.7379	76.9765	77.2079	77.4324	77.6505
3	69.7518	70.0975	70.4316	70.7548	71.0676	71.3705	71.6642	71.9490	72.2253	72.4937	72.7544
4	65.3044	65.6920	66.0670	66.4299	66.7815	67.1222	67.4526	67.7733	68.0847	68.3872	68.6813
5	61.4586	61.8798	62.2875	62.6824	63.0652	63.4364	63.7966	64.1464	64.4863	64.8166	65.1380
6	58.0430	58.4918	58.9264	59.3477	59.7563	60.1528	60.5378	60.9118	61.2755	61.6291	61.9733
7	54.9550	55.4267	55.8839	56.3273	56.7575	57.1754	57.5813	57.9759	58.3597	58.7331	59.0967
8	52.1270	52.6180	53.0942	53.5564	54.0051	54.4411	54.8649	55.2771	55.6782	56.0687	56.4491
9	49.5117	50.0191	50.5115	50.9897	51.4543	51.9059	52.3451	52.7725	53.1886	53.5939	53.9889
10	47.0744	47.5958	48.1022	48.5941	49.0723	49.5374	49.9900	50.4306	50.8598	51.2780	51.6857

TABLE 8. - SPHERICAL VOID MODEL SENSITIVITY ANALYSIS OF ILSS AS FUNCTION OF FIBER AND VOID CONTENT
[Calculated by using equation (5).]

Void volume, V_v , percent	Fiber volume, V_f , percent										
	60	59	58	57	56	55	54	53	52	51	50
	Interlaminar shear strength, percent of initial ILSS										
0	100.0000	100.0000	100.0000	100.0000	100.0000	100.0000	100.0000	100.0000	100.0000	100.0000	100.0000
1	92.0682	91.9787	91.8868	91.7921	91.6946	91.5942	91.4907	91.3839	91.2738	91.1600	91.0425
2	87.3231	87.1801	87.0331	86.8818	86.7261	86.5656	86.4001	86.2295	86.0534	85.8716	85.6838
3	83.2778	83.0893	82.8954	82.6958	82.4903	82.2786	82.0604	81.8353	81.6030	81.3632	81.1154
4	79.6096	79.3797	79.1432	78.8999	78.6493	78.3912	78.1251	77.8506	77.5674	77.2750	76.9728
5	76.1857	75.9172	75.6411	75.3569	75.0642	74.7627	74.4520	74.1314	73.8007	73.4591	73.1062
6	72.9357	72.6306	72.3167	71.9937	71.6611	71.3185	70.9653	70.6010	70.2251	69.8370	69.4359
7	69.8164	69.4762	69.1261	68.7659	68.3950	68.0128	67.6190	67.2127	66.7935	66.3606	65.9133
8	66.7994	66.4251	66.0401	65.6439	65.2359	64.8155	64.3823	63.9354	63.4743	62.9981	62.5062
9	63.8645	63.4571	63.0380	62.6068	62.1627	61.7052	61.2337	60.7473	60.2454	59.7272	59.1917
10	60.9968	60.5571	60.1048	59.6393	59.1600	58.6662	58.1572	57.6323	57.0906	56.5312	55.9532

TABLE 9. - ICAN PREDICTION OF
ROOM-TEMPERATURE ILSS FOR
COMPOSITES WITH
DIFFERENT VOID
FRACTIONS

Void content, percent	Interlaminar shear strength, ILSS	
	MPa	ksi
0	57.9	8.4
1	47.6	6.9
2	42.7	6.2
4	35.8	5.2
6	30.3	4.4
8	24.8	3.6
10	20.0	2.9

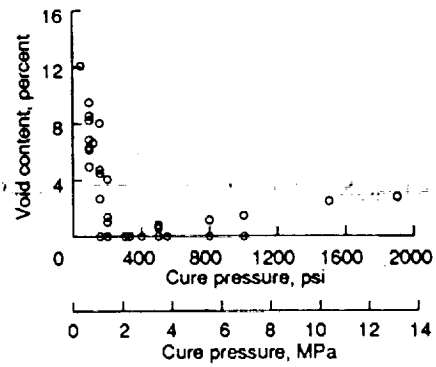


Figure 1.—Composite void content as a function of cure pressure.

ORIGINAL PAGE
BLACK AND WHITE PHOTOGRAPH

F Flexure
I Impact
T Tensile
SB Short beam shear
J-Q Spare SB
R-Y Density and micros

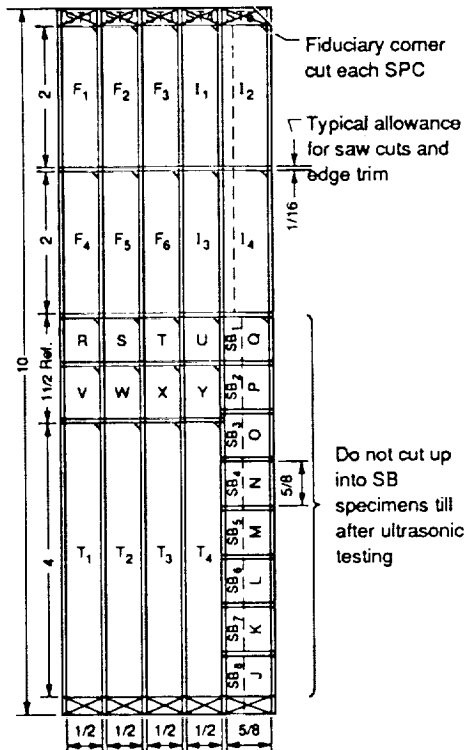
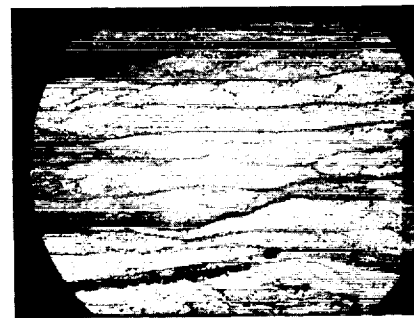
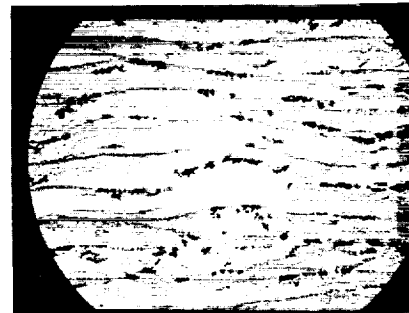


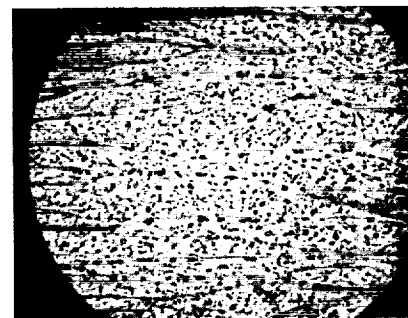
Figure 2.—Specimen excision schematic for longitudinal series 1-12 and 31-48. Dimensions are in inches.



(a) 1.25 percent voids.



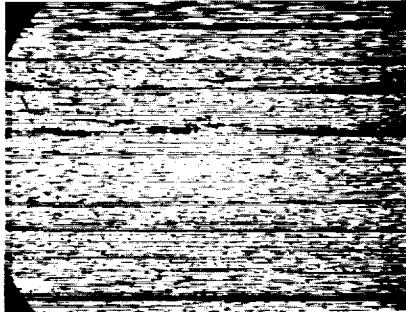
(b) 3.9 percent voids.



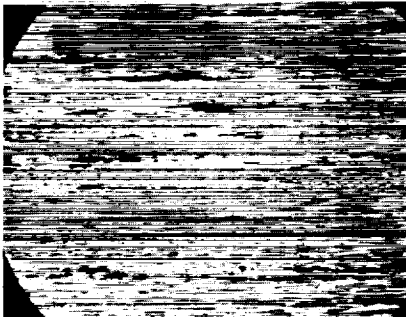
(c) 12.1 percent voids.

Figure 3.—Fiber-end views of composites.

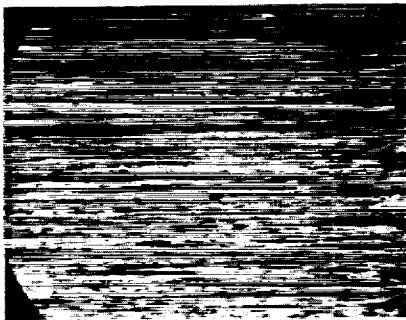
ORIGINAL PAGE
BLACK AND WHITE PHOTOGRAPH



(a) 1.25 percent voids.



(b) 3.9 percent voids.



(c) 12.1 percent voids.

Figure 4.—Fiber-side view of composites.

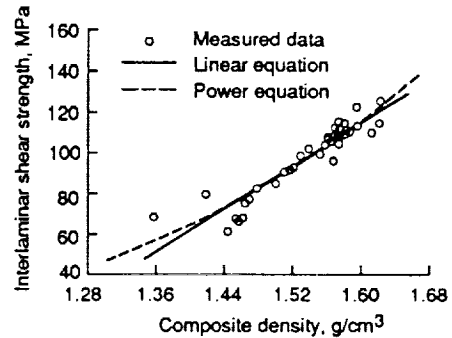


Figure 5.—Interlaminar shear strength as a function of composite density for AS4/PMR-15 unidirectional composites.

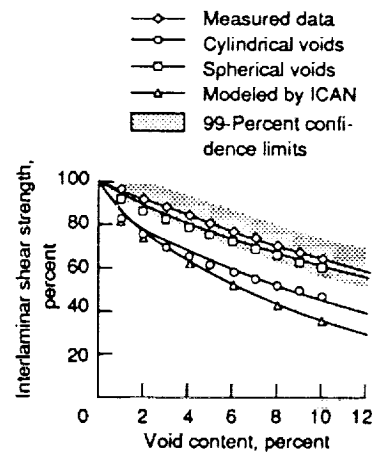


Figure 6.—Interlaminar shear strength as a function of void content for 60-percent fiber volume fraction of AS4/PMR-15 unidirectional composites.



National Aeronautics and
Space Administration

Report Documentation Page

1. Report No. NASA TM-103643	2. Government Accession No.	3. Recipient's Catalog No.	
4. Title and Subtitle Relationship Between Voids and Interlaminar Shear Strength of Polymer Matrix Composites		5. Report Date	
		6. Performing Organization Code	
7. Author(s) Kenneth J. Bowles and Stephen Frimpong		8. Performing Organization Report No. E-5825	
		10. Work Unit No. 510-01-50	
9. Performing Organization Name and Address National Aeronautics and Space Administration Lewis Research Center Cleveland, Ohio 44135-3191		11. Contract or Grant No.	
		13. Type of Report and Period Covered Technical Memorandum	
12. Sponsoring Agency Name and Address National Aeronautics and Space Administration Washington, D.C. 20546-0001		14. Sponsoring Agency Code	
15. Supplementary Notes Prepared for the 36th International SAMPE Symposium and Exhibition sponsored by the Society for the Advancement of Materials and Process Engineering, San Diego, California, April 15-18, 1991.			
16. Abstract <p>This paper describes the effect of voids on the interlaminar shear strength of a polyimide matrix composite system. The AS4 graphite/PMR-15 composite was chosen for study because this system can be readily processed by using the standard specified cure cycle to produce void-free composites and because preliminary work in this study had shown that the processing parameters of this resin matrix system can be altered to produce cured composites of varying void contents. Thirty-eight 12-ply unidirectional composite panels were fabricated for this study. A significant range of void contents (0 to 10 percent) was produced. The panels were mapped, ultrasonically inspected, and sectioned into interlaminar shear, flexure, and fiber content specimens. The density of each specimen was measured and interlaminar shear and flexure strength measurements were then made. The fiber content was measured last. The results of these tests were evaluated by using ultrasonic results, photomicrographs, statistical methods, theoretical relationships derived by other investigators, and comparison of the test data with the Integrated Composite Analyzer (ICAN) computer program developed at the Lewis Research Center for predicting composite ply properties. The testing program is described in as much detail as possible in order to help others make realistic comparisons.</p>			
17. Key Words (Suggested by Author(s)) Composites; Voids; Interlaminar shear; Graphite fibers; Polyimides; Density		18. Distribution Statement Unclassified—Unlimited Subject Category 24	
19. Security Classif. (of this report) Unclassified	20. Security Classif. (of this page) Unclassified	21. No. of pages 20	22. Price* A03

